Available online at www.sciencedirect.com
SCIENCE DIRECT®
Journal of Solid State Chemistry 177 (2004) 1667–1671
JOURNAL OF SOLID STATE CHEMISTRY
http://elsevier.com/locate/jssc

Temperature-induced phase transitions in $BaTbO_3$

W.T. Fu,[a,*] D. Visser,[b] K.S. Knight,[c] and D.J.W. IJdo[a]

[a] *Leiden Institute of Chemistry, Gorlaeus Laboratories, Leiden University, P.O. Box 9502, 2300 RA Leiden, The Netherlands*
[b] *NWO Physics, ISIS Facility, Rutherford Appleton Laboratory, Chilton, Didcot OX11 0QX, UK*
[c] *ISIS Facility, Rutherford Appleton Laboratory, Chilton, Didcot OX11 0QX, UK*

Received 11 November 2003; received in revised form 12 December 2003; accepted 17 December 2003

Abstract

The crystal structures of $BaTbO_3$ have been investigated over a wide temperature range between 40 and 773 K using high-resolution time-of-flight neutron powder diffraction. Two-phase transitions were observed. Below about 280 K, $BaTbO_3$ adopts an orthorhombic perovskite structure (space group *Ibmm*), which is characterized by rotation of TbO_6 octahedra about the pseudocubic two-fold axis. Above 280 K, $BaTbO_3$ undergoes a first-order phase transition to a tetragonal symmetry (space group $I4/mcm$), in which the tilting of the octahedra is around the pseudocubic four-fold axis. As the temperature is further increased, $BaTbO_3$ adopts the primitive cubic aristotype at about 623 K. This later phase transformation is characterized by a gradual decrease of the rotation angle, indicating a continuous phase transition, which is described by a critical exponent $\beta = 0.35$.

Keywords: High-resolution neutron powder diffraction; Crystal structure; Phase transition

1. Introduction

Many ternary compounds with the general formula ABX_3 belong to the perovskite family. The structure of the perovskites has been studied over many years because of scientific as well as technological importance. Depending on the tolerance factor, $t = (r_A + r_B)/2^{1/2}(r_B + r_X)$, where r_A, r_B and r_X are the constituent ionic radii, the perovskites may have a simple cubic structure ($t \approx 1$), space group $Pm\bar{3}m$, or a distorted one ($t > 1$ or < 1), with lower symmetry. By simple tilting of rigid BX_6 octahedra of the cubic aristotype, Glazer [1,2] developed a description of the different tilting patterns in terms of compound tilts around the pseudocubic axes, and obtained 23 corresponding space groups. Recently, Howard and Stokes [3] undertook a group-theoretical analysis and found 15 possible structures under the same conditions of tilting rigid octahedra. This analysis indicates also the possible pathways by which phase transitions occurring in perovskites might be either continuous or discontinuous.

For many distorted perovskites, increasing temperature generally has the effect of decreasing the tilt angles as was described long ago by Megaw [4], and, consequently, structural phase transitions may be expected to occur. In the past few years, temperature-induced structural phase transitions have been reported for $SrZrO_3$ [5,6], $SrHfO_3$ [7] and $SrRuO_3$ [8,9]. These compounds, with tolerance factor (t) of 0.947, 0.952, and 0.994, respectively, all have the orthorhombic $GdFeO_3$ structure, with the space group *Pbnm* (tilting $(a^-a^-c^+)$ in Glazer's notation), at low temperature, and show, by increasing temperature, a sequence of phase transitions from orthorhombic to tetragonal and, then, to the cubic aristotype.

For some $BaBO_3$-type perovskites, the tolerance factor is very close to 1, and they adopt the simple cubic structure at room temperature. Examples are $BaZrO_3$ ($t = 1.00$), $BaHfO_3$ ($t = 1.01$) and $BaSnO_3$ ($t = 1.02$). On the other hand, $BaPbO_3$ ($t = 0.98$) and $BaCeO_3$ ($t = 0.94$) have the orthorhombic structure, with space group *Ibmm* [10–12] and *Pbnm* [13], respectively. The later compound also shows a more complicated phase transition sequence of $Pbnm \rightarrow Ibmm \rightarrow R\bar{3}c \rightarrow Pm\bar{3}m$, with increasing temperature [13].

$BaTbO_3$ ($t = 0.985$) is known to be a distorted perovskite. The structure of this compound, both at room temperature and at 4 K, was first determined from powder neutron diffraction data by Jacobson et al. [14,15], to be rhombohedral (space group $R\bar{3}c$, tilting $(a^-a^-a^-)$ in Glazer's notation). Banks et al. [16] also

*Corresponding author. Fax: 31-71-5274537.
E-mail address: w.fu@chem.leidenuniv.nl (W.T. Fu).

0022-4596/$ - see front matter © 2004 Published by Elsevier Inc.
doi:10.1016/j.jssc.2003.12.022

found the same space group from the powder neutron diffraction data. Recently, Tezuka et al. [17] have reported an orthorhombic space group *Pbnm* for $BaTbO_3$ (tilting ($a^-a^-c^+$)), as was obtained from high-resolution powder neutron diffraction data. However, the present authors have shown, by using high-resolution powder neutron diffraction, that the room-temperature structure of $BaTbO_3$ is actually tetragonal with the space group $I4/mcm$ (tilting ($a^0a^0c^-$)) [18].

The present investigation is devoted to the study of the phase transitions that may occur in $BaTbO_3$. Since the tolerance factor of $BaTbO_3$ is close to unity and is only slightly larger than that of $BaPbO_3$, one may expect structural phase transitions in $BaTbO_3$ as a function of temperature. We have, therefore, carried out a crystal structure study over a wide temperature range using high-resolution time-of-flight powder neutron diffraction technique, and report the results in this paper.

2. Experimental

A powder sample of $BaTbO_3$ was prepared from AR $BaCO_3$ and Tb_4O_7 (99.99%) in an alumina crucible. The mixture was intimately ground and heated in air at 1323 K for 2 weeks with repeated grindings, followed by furnace cooling to room temperature.

X-ray diffraction patterns were collected with a Philips PW1050 diffractometer using monochromatic Cu$K\alpha$ radiation in the range of $10° < 2\theta < 117°$ with the step size of 0.02° and 12 s counting time at each step. High-resolution time of fight powder neutron diffraction data were obtained at the HRPD diffractometer, ISIS Facility, Rutherford Appleton Laboratories. The sample was loaded into a 11 mm diameter vanadium can and placed either in a cryostat ($T < 300$ K) or in a furnace ($T \geqslant 300$ K). The diffraction patterns were recorded in both the backscattering bank and the 90° detector bank, over the time-of-flight range 32–120 and 35–114 ms, corresponding to the d spacings from 0.6–2.5 to 1.0–3.3 Å, respectively. The patterns were normalized to the incident beam spectrum as recorded in the upstream monitor, and corrected for detector efficiency according to prior calibration with vanadium (rod). Most patterns were recorded to a total incident proton beam of about 120 μA h, for approximately 4 h. Calculations were performed simultaneously on both backscatterings and 90° bank data by the Rietveld method using the GSAS computer program [19].

3. Results

The X-ray diffraction pattern of $BaTbO_3$ at room temperature revealed a single phase, which could be interpreted with the distorted perovskite structure with a supercell of cell dimensions: $a \approx b \approx \sqrt{2}a_0$ and $c \approx a_0$, where a_0 is the cell parameter of the ideal cubic perovskite.

The refinement of neutron powder diffraction data above the room temperature was carried out in the space group $I4/mcm$ as reported earlier [18]. Examination of the high-resolution backscattering data at 623 K has shown, however, the disappearance of the superlattice reflections as well as the splittings of basic reflections of perovskite (Fig. 1a). Consequently, the structure of $BaTbO_3$ was modelled with the simple cubic perovskite in the space group $Pm\bar{3}m$. During the refinements, we observed a few weak reflections at the d value of about 2.06, 1.78 and 1.26 Å, respectively. These weak reflections do not, however, show up in our low-temperature data. Careful analysis has shown that they are due to the chromel–alumel thermocouple that was placed outside the vanadium can. Since the exact composition is not known, and the attempt of introducing nickel as the second phase did not affect the refinement results, we did not consider these reflections further in the refinements.

Below room temperature, at about 280 K, a phase transition to an orthorhombic structure is observed as indicated by the splitting of the (400) reflection of the tetragonal phase (Fig. 1b). Since no additional reflections, resulting from the coupled in-phase tilting around the pseudocubic $[001]_p$-axis, were observed, we

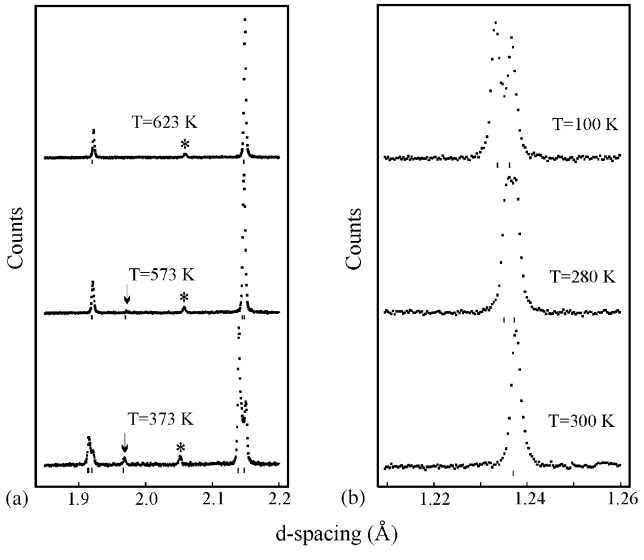

Fig. 1. A section of the observed high-resolution neutron diffraction patterns of $BaTbO_3$ at some representative temperatures. In (a), both the splitting of main diffraction peaks and the superlattice diffraction (indicated by the arrow) can be seen. A small peak due to the contamination of chromel–alumel thermocouple is shown by *. (b) Basic (222) diffraction, which remains single line in $I4/mcm$ and splits into two in *Ibmm*. Note that the splitting starts already at $T = 280$ K. Tick marks below indicate the allowed diffraction by each space group (see also the discussion in the text).

Table 1
Refined atomic positions and thermal parameters of $BaTbO_3$ at some selected temperatures

T (K)	40	100	260	373	473	573	623	873
Space group	*Ibmm*			*I4/mcm*			*Pm*$\bar{3}$*m*	
a (Å)	6.07141(10)	6.07123(10)	6.07202(13)	6.05275(4)	6.06175(3)	6.07110(5)	4.29692(1)	4.30226(1)
b (Å)	6.04407(10)	6.04591(10)	6.05519(13)					
c (Å)	8.52560(13)	8.52897(13)	8.54526(16)	8.59573(8)	8.59598(8)	8.59512(14)		
Tb	4*a* (0,0,0)			4*c*(0, 0, 0)			1*a*(0, 0, 0)	
U^*_{iso}	0.12(4)	0.11(4)	0.27(4)	0.14(3)	0.29(3)	0.36(3)	0.45(3)	0.58(3)
Ba	4*e*(x, 0, 1/4)			4*b*(1/2, 0, 1/4)			1*b*(1/2, 1/2, 1/2)	
	x: 0.5015(7)	0.5009(7)	0.4985(11)					
U^*_{iso}	0.50(4)	0.56(4)	0.98(5)	1.00(4)	1.29(4)	1.54(4)	1.65(4)	2.08(5)
O(1)	4*e*(x, 0, 1/4)			4*a*(0, 0, 1/4)			3*d*(1/2, 0, 0)	
	x: 0.0525(4)	0.0508(4)	0.0449(6)					
U^*_{iso}	0.73(8)	0.83(8)	1.32(11)	1.63(7)	2.17(10)	2.65(22)	2.81(4)	3.07(4)
O(2)	8*g*(1/4, 1/4, z)			8*h*(x, 1/2 + x, 0)				
	z: −0.0282(2)	−0.0273(2)	−0.0238(3)	x: 0.2780(1)	0.2730(2)	0.2657(2)		
U^*_{iso}	0.71(5)	0.85(5)	1.42(7)	1.41(4)	1.87(5)	2.29(11)		
R_{wp} (%)	8.34	8.00	8.54	6.33	6.09	6.57	6.73	6.89
R_p (%)	6.48	6.25	6.38	5.39	5.17	5.47	5.46	5.66

$U^*_{iso} = U_{iso} \times 100$.

concluded that this orthorhombic phase belongs to the space group *Ibmm* ($a^-a^-c^0$). It is worth mentioning that this phase transition, although clearly visible at 280 K, shows hysteresis and exhibits a small two-phase region, $\Delta T \sim 10$ K. For example, the refinement of neutron diffraction data at 280 K in the space group $I4/mcm$ still gives slightly lower agreement factor ($R_{wp} = 8.61\%$) than that in the space group *Ibmm* ($R_{wp} = 9.60\%$). On the other hand, full convergence could not be reached when refining the diffraction data at 260 K in $I4/mcm$, even by using the highest damping factor. It resulted also in poor agreement factor ($R_{wp} = 9.56\%$) as compared to that in the space group *Ibmm* ($R_{wp} = 8.54\%$). Below about 20 K, some magnetic diffraction lines are visible in agreement with the observations of Tezuka et al. [17].

Table 1 summarizes the refined atomic positions and the thermal parameters for $BaTbO_3$ at selected temperatures. Fig. 2 shows a few examples of the observed and calculated profiles.

4. Discussion

At low temperature, the structure of $BaTbO_3$ has the space group *Ibmm* ($a^-a^-c^0$), which can be derived from the cubic aristotype by tilting the octahedra around the primitive $[110]_p$-axis. The tilting angle decreases smoothly with increasing temperature ranging from 9.0–7.2° at 40 and 260 K, respectively (Fig. 3). The a-axis remains nearly constant whereas the b- and c-axis expand with rising temperature (Fig. 4). The observed space group *Ibmm* is in agreement with the powder neutron diffraction diagram at 10 K of Tezuka et al. [17], which shows the absence of reflections for

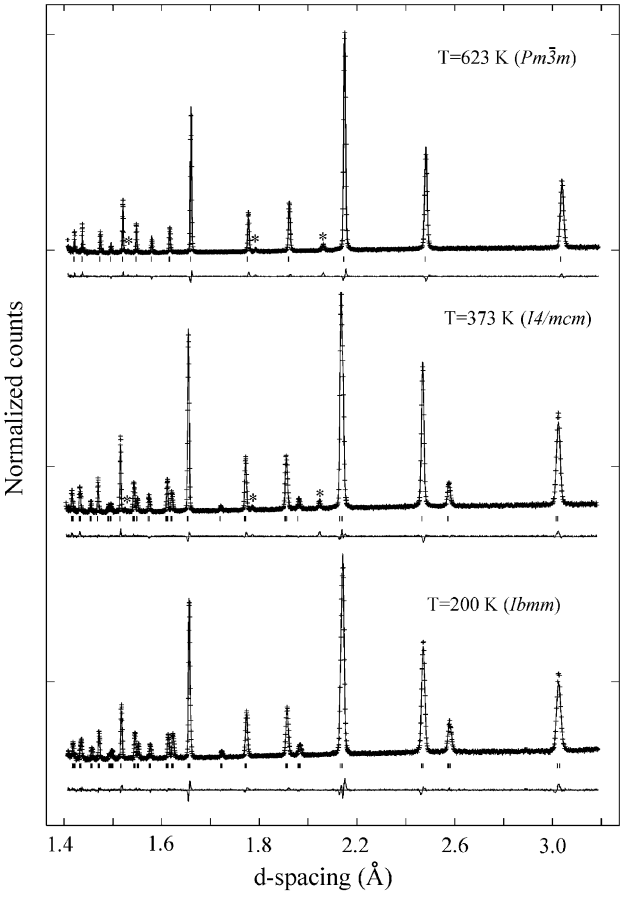

Fig. 2. Observed (crosses) and calculated (continuous line) profiles (90° bank data) of $BaTbO_3$ at $T = 200$, 375 and 635 K in the space groups *Ibmm*, $I4/mcm$ and $Pm\bar{3}m$, respectively. Tick marks indicate the positions of allowed reflections by each space group. The difference curve ($I_{obs.}$–$I_{cal.}$) is shown at the bottom. A few visible peaks due to the contamination of the chromel–alumel thermocouple are marked by *.

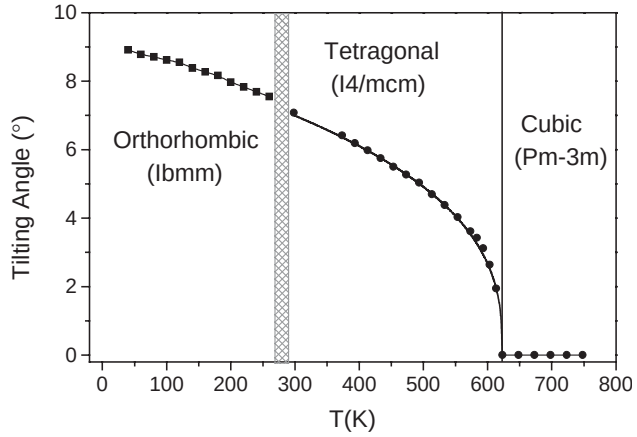

Fig. 3. Temperature dependence of the tilting angles in $BaTbO_3$. The continuous line in tetragonal phase region is the fit to the expression: $\varphi = A(T_c - T)^{\beta}$ with $\beta = 0.35$, $A = 0.90$ and $T_c = 623$ K.

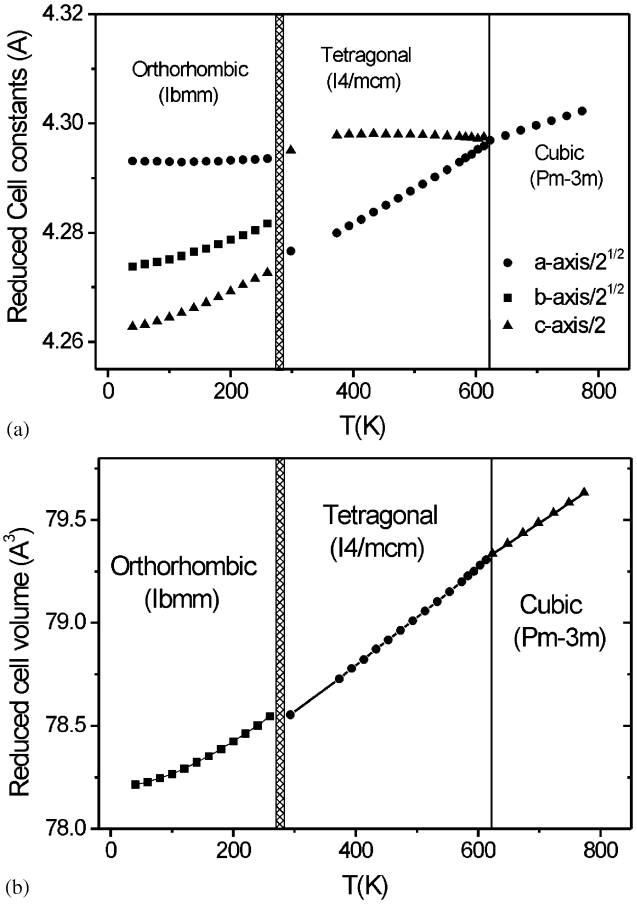

Fig. 4. Temperature dependence of (a) reduced cell constants, and (b) reduced cell volume for $BaTbO_3$. Note that the cell volume shows discontinuous change across the $Ibmm \rightarrow I4/mcm$ phase transition.

$h + k + l = 2n + 1$. This confirms an I-centered cell rather than a primitive cell.

Above about 280 K, the structure of $BaTbO_3$ becomes tetragonal with the space group $I4/mcm$, characterized by the change of c/a ratio from $c/a < 1$ to $c/a > 1$ across the phase transition. In $I4/mcm$, the TbO_6 octahedra are tilted around the primitive $[001]_p$-axis. Since it involves an abrupt change of octahedral tilting from a diad axis to a tetrad axis, the phase transition from $Ibmm$ to $I4/mcm$ is first order. A discontinuous change of the (reduced) cell volume can be clearly seen (Fig. 3) as well as a hysteresis behavior around 280 K. These observations underwrite the prediction from the group-theoretical analysis that this structural phase transition should be first order.

The tetragonal $I4/mcm$ structure persists over a relatively wide temperature range and transforms to the aristotype cubic ($Pm\bar{3}m$) at about 623 K. In agreement with the diagram of group–subgroup relation given by Howard et al. [3], both the lattice parameters and the tilting angle gradually change with the temperature (Figs. 3 and 4), suggesting that the tetragonal→cubic transition is probably continuous. To evaluate the phase transition, we have used the tilting angle (φ) as the order parameter and fitted its variation with temperature using the general form for the temperature dependence of the order parameter [20]:

$$\varphi = A(T_c - T)^{\beta},$$

where T_c ($= 623$ K) is the transition temperature, and β is termed the "critical exponent". The experimentally fitted value gives $\beta = 0.35$ with $A = 0.90$. For continuous structural phase transitions, the β-values of 0.5 and 0.25 are expected for a mean field second-order transition or a tricritical transition, respectively. No model prediction for the observed β value in $BaTbO_3$ is known. However, its value would fit in the three-dimensional Heisenberg universality class. We mention that the similar phase transition has also been observed in $SrZrO_3$ and $SrHfO_3$, but characterized by either tricritical ($\beta = 0.25$) or mean field second-order transition ($\beta = 0.50$), respectively [5,7].

The phase sequence of $Ibmm \rightarrow I4/mcm \rightarrow Pm\bar{3}m$ that occurs in $BaTbO_3$ with increasing temperature is what one would expect for a distorted perovskite in which the distortion is solely confined to the tilting of octahedra. It has already been observed in perovskites such as $SrZrO_3$ [6] and $SrRuO_3$ [8], although the $Ibmm$ phase has once been either wrongly assigned as $Cmcm$ in the former [7] or missing in the later compound [9]. We noted that a similarly high-resolution powder neutron diffraction study on $BaCeO_3$ has revealed a somewhat different sequence of phases, $Pnma \rightarrow Ibmm \rightarrow R\bar{3}c \rightarrow Pm\bar{3}m$ [13]. On the other hand, our recent study on $BaPbO_3$ has shown the same phase sequence reported here, and the detailed results will be published elsewhere.

Acknowledgments

Financial support from the Netherlands Organization for Scientific Research (NWO) for this work is gratefully acknowledged.

References

[1] A.M. Glazer, Acta Crystallogr. B 28 (1972) 3384.
[2] A.M. Glazer, Acta Crystallogr. A 31 (1975) 756.
[3] C.J. Howard, H.T. Stokes, Acta Crystallogr. B 54 (1998) 782.
[4] H.D. Megaw, Crystal Structures—A Working Approach, W.B. Saunders, Philadelphia, 1973.
[5] B.J. Kennedy, C.J. Howard, Phys. Rev. B 59 (1999) 4023.
[6] C.J. Howard, K.S. Knight, B.J. Kennedy, E. Kisi, J. Phys.: Condens. Matter 12 (2000) L677.
[7] B.J. Kennedy, C.J. Howard, B.C. Chakoumakos, Phys. Rev. B 60 (1999) 2972.
[8] B.J. Kennedy, B.A. Hunter, Phys. Rev. B 58 (1998) 653.
[9] B.J. Kennedy, B.A. Hunter, J.R. Hester, Phys. Rev. B 65 (2002) 224103.
[10] A.J. Jacobson, B.C. Tofield, B.E.F. Fender, Acta Crystallogr. B 28 (1972) 956.
[11] W.T. Fu, D.J.W. IJdo, Solid State Commun. 95 (1995) 581.
[12] S.M. Moussa, B.J. Kennedy, T. Vogt, Solid State Commun. 95 (2001) 549.
[13] K.S. Knight, Solid State Ionics 74 (1994) 109.
[14] A.J. Jacobson, B.C. Tofield, B.E.F. Fender, Acta Crystallogr B 28 (1972) 956.
[15] B.C. Tofield, A.J. Jacobson, B.E.F. Fender, J. Phys. C 5 (1972) 2887.
[16] E. Banks, S.J. La Place, W. Kunnmann, L.M. Corliss, J.M. Hastings, Acta Crystallogr. B 28 (1972) 3429.
[17] K. Tezuka, Y. Hinatsu, Y. Shimojo, Y. Morii, J. Phys.: Condens. Matter 10 (1998) 11703.
[18] W.T. Fu, D. Visser, D.J.W. IJdo, J. Solid State Chem. 165 (2002) 393.
[19] A.C. Larson, R.B. Von Dreele, GSAS general structure analysis system, Report LAUR 86-748, Los Alamos National Laboratory, Los Alamos, NM, 1986.
[20] E.K.H. Salje, Phase Transitions in Ferroelastic and Co-Elastic Crystals, Cambridge University Press, Cambridge, 1990.